

# X-ray powder diffraction and Mössbauer spectroscopic studies on the solubility limits in $\gamma$ -FeOOH/ $\gamma$ -AlOOH solid solutions

E. WOLSKA\*

*Department of Magnetochemistry, Adam Mickiewicz University, Poznań, Grunwaldzka 6, PL-60780 Poznań, Poland*

J. ŠUBRT, Z. HÁBA, J. TLÁSKAL

*Institute of Inorganic Chemistry, Czechoslovak Academy of Sciences, Prague, 250 68 Řež u Prahy, Czech Republic*

U. SCHWERTMANN

*Institute of Soil Sciences, Technical University Munich, D-8050 Freising-Weihenstephan, FGR*

The formation of substitutional solid solutions between the isostructural  $\gamma$ -FeOOH (lepidocrocite) and  $\gamma$ -AlOOH (boehmite) was investigated by X-ray powder diffraction, Mössbauer spectroscopy, electron microscopic and thermal analysis. Samples of  $\gamma$ -(Fe,Al)OOH were obtained at 15 °C and pH 8 by oxidation of mixed  $\text{FeCl}_2$ - $\text{Al}(\text{NO}_3)_3$  solutions. The unit cell parameters decreased with increasing aluminium content from  $a = 0.3072$  nm,  $b = 1.253$  nm and  $c = 0.3874$  nm, to 0.3053, 1.250 and 0.3858 nm, respectively. The temperature of the differential thermal gravimetry maximum increased with aluminium content up to 10 mol % Al. Quadrupole splitting distribution in the room temperature Mössbauer spectra showed a clear dependence on the concentration of substituted aluminium, enabling determination of the  $\gamma$ -( $\text{Fe}_{1-x}\text{Al}_x$ ) $_{1-y/3}\text{O}_{1-y}(\text{OH})_{1+y}$  solid solution limits at  $0 \leq x \leq 0.1$ . The cation deficiency in samples responded to  $y = 0.16$  over the whole range of solid solutions formed.

## 1. Introduction

Despite extensive studies of substitutional solid solutions formed between the isostructural oxides and oxyhydroxides of aluminium and iron, very few experiments on the system  $\gamma$ -FeOOH/ $\gamma$ -AlOOH (lepidocrocite/boehmite) have been carried out. One reason for this is that it is often difficult to synthesize the pure single-phase samples, either because aluminium ions induce the production of  $\alpha$ -hydroxide oxide polymorph or because the crystallinity of the product decreases with increasing aluminium content.

The isomorphous incorporation of aluminium in the lattice of soil lepidocrocites has already been suggested, based on magnetic properties of decomposition products [1] and on the X-ray powder diffraction (XRD) investigations [2–4]. Recently, a new method for the preparation of synthetic  $\gamma$ -(Fe,Al)OOH solid solutions samples enabled further studies on that system to be made, and provided evidence of the formation of limited solid solutions [5–7].

The solubility limits, however, remain as yet undetermined, despite several indications based on thermal analysis and on magnetic properties of the

$\gamma$ -(Fe,Al)OOH dehydration products,  $\gamma$ -(Fe,Al) $_2\text{O}_3$  [6, 7]. A major difficulty arises from the low crystallinity of  $\gamma$ -(Fe,Al)OOH samples containing more than 10 mol % AlOOH, making the precise determination of lattice parameters by X-ray diffraction impossible. Recent studies of Mössbauer effects of the synthetic  $\gamma$ -FeOOH revealed that neither the hyperfine field nor the Néel temperature distribution were affected by the crystallinity of samples [8]. In the present paper we present for the first time the Mössbauer spectroscopic results for synthetic  $\gamma$ -Fe $_{1-x}$ Al $_x$ OOH solid solution series and we analyse them using X-ray, electron microscopic and thermal analyses.

## 2. Experimental procedure

A series of aluminium-substituted  $\gamma$ -iron hydroxide oxides was prepared following the method described previously [5].

The gravimetric determination of H $_2$ O content was based on the thermogravimetric (TG) and differential thermogravimetric (DTG) curves recorded on a Shimadzu TGA 50 instrument. X-ray powder diffraction studies were performed on TUR-61 (HZG-3) unit and

\* Author to whom all correspondence should be addressed.

on a Huber-Guinier 600 (type 642) diffractometer using  $\text{CoK}_\alpha$  radiation. Micrographs of preparations were obtained with a transmission electron microscope, TESLA BS 242 E. Absorption  $^{57}\text{Fe}$  Mössbauer spectra were recorded on a 500 channels conventional spectrometer. For velocity scale calibration and as an isomer shift standard,  $8\text{ }\mu\text{m}$   $\alpha\text{-Fe}$  foil was used.

### 3. Results and discussion

The oxidation of mixed  $\text{FeCl}_2$  and  $\text{Al}(\text{NO}_3)_3$  solutions at pH 8 at a temperature of  $13\text{--}15^\circ\text{C}$  [5] yielded  $\gamma\text{-Fe}_{1-x}\text{Al}_x\text{OOH}$  solid solution samples showing the orthorhombic lepidocrocite structure (space group  $\text{Cmcm}$ ), well crystallized for  $0 \leq x \leq 0.1$ . For higher aluminium content, the crystallinity decreased distinctly and preparations with  $x > 0.2$  were nearly amorphous (Fig. 1).

The two-stage thermal dehydration during the gravimetric determination of  $\text{H}_2\text{O}$  content in samples was carried out in order first to eliminate at  $150^\circ\text{C}$  the water adsorbed and/or contained in the amorphous  $(\text{Fe,Al})(\text{OH})_3$ , and then to remove at  $1000^\circ\text{C}$  the constitutional water of aluminium lepidocrocites. Results presented in Fig. 2 point to the nonstoichiometry of  $\gamma\text{-(Fe,Al)OOH}$  samples [9], because the structural water content, after preheating at  $150^\circ\text{C}$ , exceeds that in the formula  $\text{Fe}_{1-x}\text{Al}_x\text{OOH}$  ( $\text{OH}^-/\text{O}^{2-} = 1$ ) and responds to the  $\text{OH}^-/\text{O}^{2-}$  ratio of about 1.38, i.e. to  $y = 0.16$  in the general formula  $\gamma\text{-(Fe}_{1-x}\text{Al}_x)_{1-y/3}\text{O}_{1-y}(\text{OH})_{1+y}$ .

The increase in aluminium content did not influence, however, the degree of cation deficiency in the

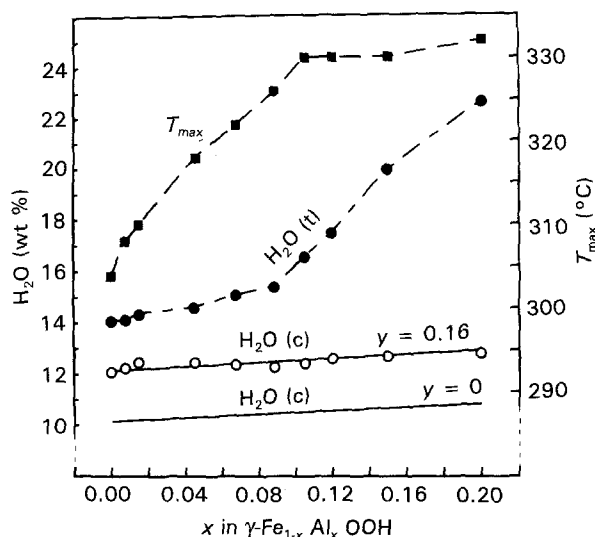


Figure 2 Temperatures of the DTG peaks ( $T_{\max}$ ) from the lepidocrocite  $\rightarrow$  maghaemite transition and the  $\text{H}_2\text{O}$  content in the  $\gamma\text{-(Fe}_{1-x}\text{Al}_x)_{1-y/3}\text{O}_{1-y}(\text{OH})_{1+y}$  samples plotted against the aluminium content. ( $\text{H}_2\text{O}_{(t)}$ ) total, and ( $\text{H}_2\text{O}_{(c)}$ ) constitutional water. (—)  $\text{H}_2\text{O}$  content calculated for  $y = 0$  and  $0.16$ .

lepidocrocite structure and the composition responding to the formula of  $(\text{Fe}_{1-x}\text{Al}_x)_{0.95}\text{O}_{0.84}(\text{OH})_{1.16}$  was found in all series of samples for  $0 \leq x \leq 0.2$ . It was previously stated that, for example, in the aluminium hydrohaematite and aluminium goethite solid solutions, the aluminium substitution affects the hydroxylation of anionic sublattices and enhances the cation vacancies [10, 11]. Thermogravimetric analysis shows that thermal stability of the aluminium-substituted

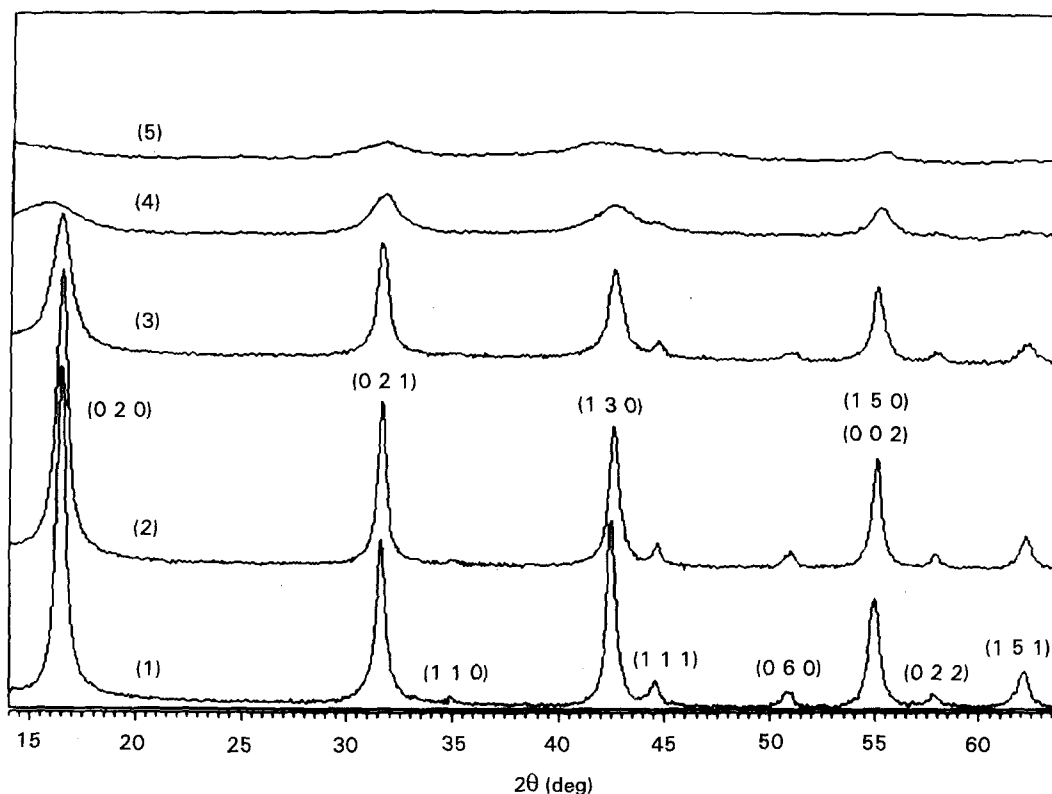


Figure 1 X-ray powder diffraction patterns of synthetic samples of the aluminium-substituted lepidocrocites,  $\gamma\text{-Fe}_{1-x}\text{Al}_x\text{OOH}$ , with  $x =$  (1) 0.00, (2) 0.0525, (3) 0.105, (4) 0.15 and (5) 0.20.

lepidocrocites increases with the increasing aluminium content. The plot of the maxima of DTG peaks,  $T_{\max}$ , against aluminium content, in Fig. 2, demonstrates that the temperature of the transformation reaction  $\gamma\text{-(Fe,Al)OOH} \rightarrow \gamma\text{-(Fe,Al)}_2\text{O}_3$  rises for  $0 \leq x \leq 0.1$ , confirming indirectly the existence of a solubility limit of aluminium at about 10 mol %.

The precise determination of lattice constants of the orthorhombic unit cell of aluminium lepidocrocites, based on the positions of (0 2 1), (1 3 0), (0 0 2), (0 2 3), (1 5 1), (0 8 0), (2 0 0), (1 3 2), and (1 7 1) X-ray reflections, was performed with the aid of a fitting program employed at the Institute of Soil Sciences, TU Munich [5]. Results are presented in Fig. 3, compared to the Vegard's law predictions for the  $\text{AlOOH/FeOOH}$  solid solutions. The sudden break in crystallinity, when the aluminium content in the samples exceeds 10 mol %, makes it impossible to define the exact value of  $x_{\max}$  in  $(\text{Fe}_{1-x}\text{Al}_x)_{1-y/3}\text{O}_{1-y}(\text{OH})_{1+y}$  but, on the other hand, suggests the destructive role of the surplus, not incorporated aluminium, appearing as a separate, non-crystalline aluminium hydroxide phase, in the formation of crystalline lepidocrocite structure.

Electron micrographs (Fig. 4) show the typical morphology of lepidocrocite to consist of plates having strongly serrated edges in the  $z$ -direction. The crystallinity of samples is closely correlated with the aluminium content. With increasing substitution, this morphology is less well expressed and the crystals are considerably smaller in length and width. To determine the thickness of the crystals, which cannot be seen from the micrographs, the mean crystallite dimension along the  $b$ -axis ( $\text{MCD}_b$ ) was estimated from the width at half intensity of the (0 2 0) X-ray reflection using Scherrer's formula. With increasing aluminium

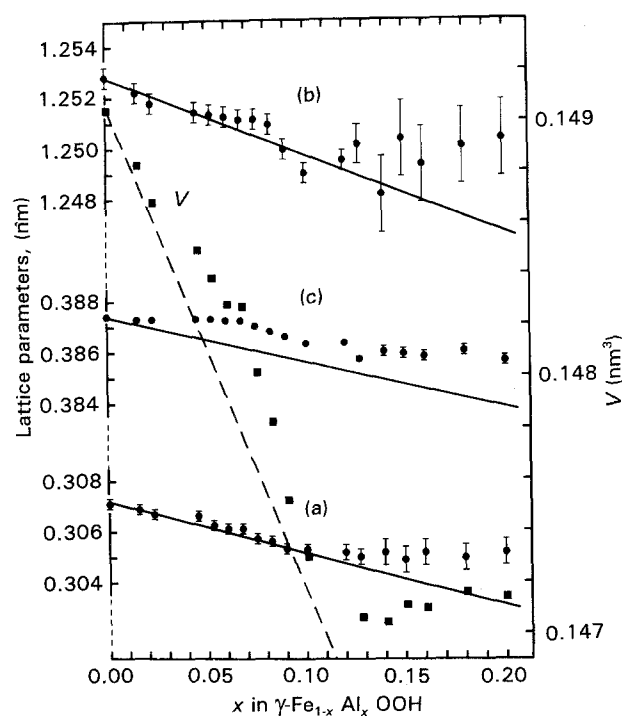


Figure 3 Lattice constants  $a$ ,  $b$  and  $c$ , and the unit cell volume of aluminium-substituted lepidocrocites, as a function of aluminium content. (—) The Vegard's law behaviour.

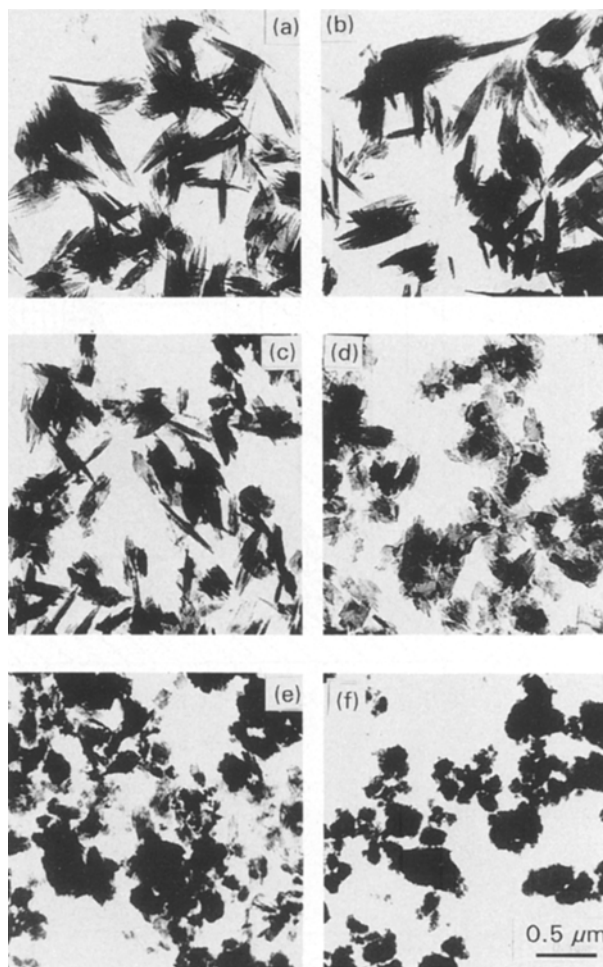


Figure 4 Electron micrographs of synthetic aluminium-substituted lepidocrocites with  $x =$  (a) 0.00, (b) 0.015, (c) 0.03, (d) 0.06, (e) 0.9 and (f) 0.40, in  $\gamma\text{-Fe}_{1-x}\text{Al}_x\text{OOH}$ .

substitution from 0–12.5 mol %,  $\text{MCD}_b$  decreased from 0.27  $\mu\text{m}$  to 0.031  $\mu\text{m}$ , indicating a very strong inhibitory effect of structural aluminium on crystal growth perpendicular to the zig-zag layers.

In order to catch the influence of possibly small aluminium substitution on the room-temperature (RT) Mössbauer spectra of lepidocrocite, the high quality spectra in the velocity range  $\pm 3 \text{ mm s}^{-1}$  were measured. The careful analysis was based on the model consisting of two background components and the lepidocrocite doublet with distribution of quadrupole splitting (QS). The measurements were made in the concentration range 0–20 mol % aluminium. Examples of QS distributions are given in Fig. 5. The shape of the distribution for pure lepidocrocite, in agreement with other authors [8, 12], is formed by two distinct peaks. The main peak can be attributed to the bulk material. According to Vandenberghe *et al.* [13], the satellite peak originates from the surface layers, especially from the region of strongly serrated edges (experiments with the removal of the sawtooth part by means of hot KOH containing silicon resulted in a decrease of surface area from  $65 \text{ m}^2 \text{ g}^{-1}$  to  $18 \text{ m}^2 \text{ g}^{-1}$  and it was possible to fit the RT spectrum of lepidocrocite with only one doublet with relatively small linewidth of  $0.26 \text{ mm s}^{-1}$ ).

Aluminium substitution affects the appearance of QS distribution significantly from a concentration of

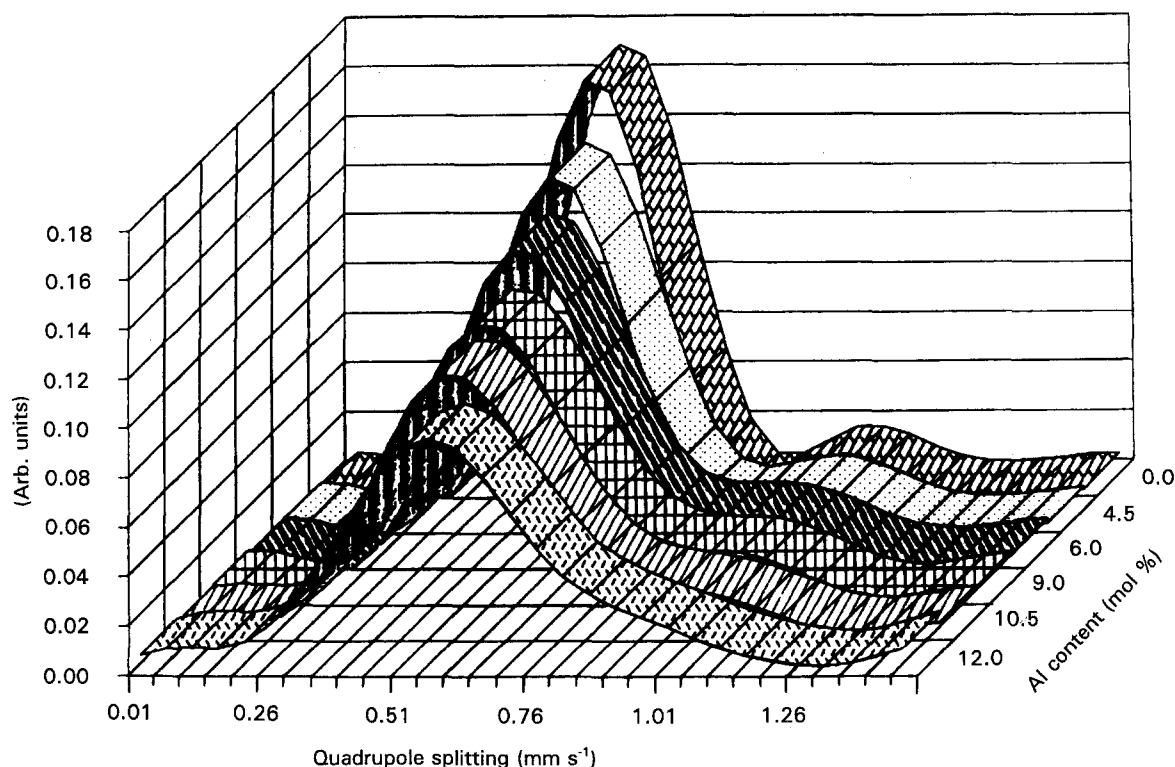


Figure 5 Distributions of quadrupole splitting in the room-temperature Mössbauer spectra for  $\gamma\text{-Fe}_{1-x}\text{Al}_x\text{OOH}$  samples with different aluminium contents ( $x \cdot 100\% = \text{mol } \%$ ).

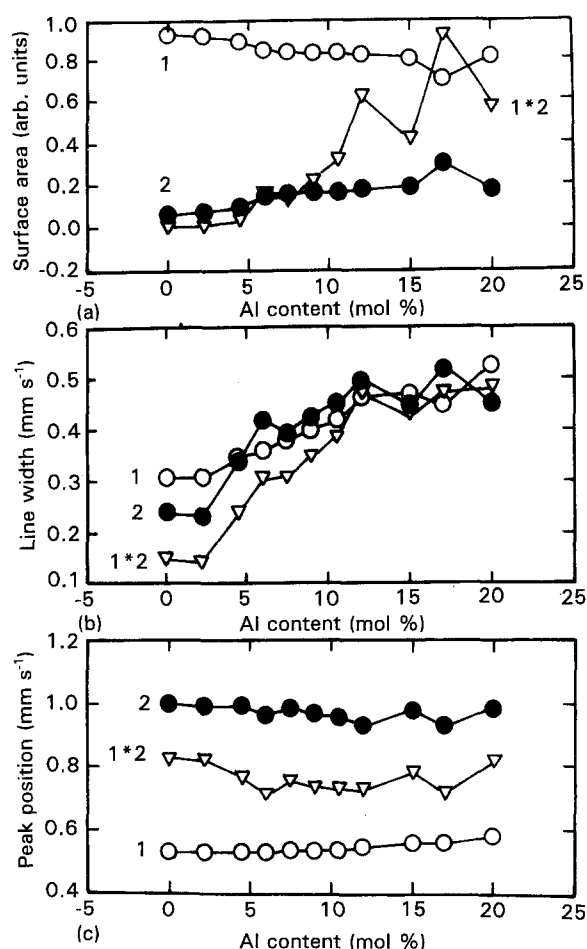


Figure 6 The effect of aluminium concentration on the distribution of QS in the Mössbauer spectra of  $\gamma\text{-Fe}_{1-x}\text{Al}_x\text{OOH}$ : variation of (a) surface area, (b) line width and (c) position of peaks. Curve 1, (○) Main gaussian peak; Curve 2, (●) satellite gaussian peak; Curve 1\*2, (△) the product of Curves 1 and 2; see text.

more than 2 mol % Al. In order to describe these changes quantitatively, the distribution peaks were fitted with gaussian lines. The resulting parameters are summarized in Fig. 6, where Curve 1 is for the main gaussian peak, Curve 2 for the satellite gaussian peak and Curve 1\*2 for the product of both (indicating overlapping of the first two gaussians).

The distribution shape is supposed to be affected by the crystallinity of samples and the aluminium content. The influence of crystallinity is not quite clear, in addition to the fact that smoothing of the edges is accompanied by a decrease in thickness of the crystallites. However, a mild increase of "surface" peak area can be seen. The substitution of smaller  $\text{Al}^{3+}$  for the  $\text{Fe}^{3+}$  ions affects the structure in some way, and thus we can expect a QS distribution broadening, because it illustrates the gaussian width dependence in the interval of 2–12 mol % Al content. As the aluminium concentration grows, the original picture of two distinct peaks is replaced by one asymmetrical maximum, typical for highly disordered material such as ferrihydrite (see [8]). These two overlapping peaks dramatically increase behind the 10 mol % Al substitution, as is shown in the plot of product area in Fig. 6.

#### 4. Conclusions

Results of joint X-ray diffraction and Mössbauer spectroscopic studies on the synthetic substitutional solid solutions formed in the  $\gamma\text{-FeOOH}/\gamma\text{-AlOOH}$  system demonstrate that the solubility limit of aluminium ions in the orthorhombic  $\gamma\text{-FeOOH}$  lattice may be fixed at about 10 mol % Al. The surplus  $\text{Al}^{3+}$  ions coprecipitated with iron ions during preparation

but not incorporated into the lepidocrocite structure, strongly affect the crystallinity of the samples, which results in the formation of X-ray amorphous ferrihydrite for higher aluminium content. Contrary to the solid solutions of other (Fe,Al) oxides and hydroxides, the increase in aluminium content does not enhance the hydroxylation of the anionic sublattice and about the same cation deficiency appears over the whole range of solid solution formed.

### Acknowledgments

E. W. thanks DAAD (FRG) for a fellowship, which helped to realize this project. The authors also thank Dr J. Kaczmarek and M.Sc. P. Piszora, for technical assistance.

### References

1. J. M. de VILLIERS and T. H. van ROOYEN, *Clay Miner.* **7** (1967) 229.
2. R. M. TAYLOR and U. SCHWERTMANN, *Clays Clay Miner.* **28** (1980) 267.
3. C. W. CHILDS and A. D. WILSON, *Aust. J. Soil Res.* **21** (1983) 489.
4. R. W. FITZPATRICK, R. M. TAYLOR, U. SCHWERTMANN and C. W. CHILDS, *ibid.* **23** (1985) 543.
5. U. SCHWERTMANN and E. WOLSKA, *Clays Clay Miner.* **38** (1990) 209.
6. E. WOLSKA, W. SZAJDA and P. PISZORA, *J. Therm. Anal.* **38** (1992) 2115.
7. E. WOLSKA, *Solid State Ionics* **44** (1990) 119.
8. E. de GRAVE, R. M. PERSOONS, D. G. CHAMBAERE, R. E. VANDENBERGHE and L. H. BOWEN, *Phys. Chem. Miner.* **13** (1986) 61.
9. E. WOLSKA and J. BASZYŃSKI, *Phys. Status Solidi (a)* **95** (1986) 87.
10. H. STANJEK and U. SCHWERTMANN, *Clays Clay Miner.* **40** (1992) 347.
11. E. WOLSKA and U. SCHWERTMANN, *N. Jb. Miner. Mh.* **5** (1993) 213.
12. J. ŠUBRT, F. HANOUSEK, V. ZAPLETAL, J. LIPKA and M. HUCL, *J. Therm. Anal.* **20** (1981) 61.
13. R. E. VANDENBERGHE, E. de GRAVE, C. LANDUYDT and L. H. BOWEN, *Hyperfine Interactions* **53** (1990) 175.

*Received 26 May  
and accepted 16 December 1993*